

## ***Supplementary Material***

### **Improved photo-dechlorination at polar photocatalysts $K_3B_6O_{10}X$ ( $X = Cl, Br$ ) by halogen atoms-modulated surface polarization**

Yang Zhang <sup>a, b</sup>, Xiaoyun Fan <sup>b\*</sup>, Yang Yu <sup>b</sup>, Yufei Zhai <sup>c</sup>, Zhi Su <sup>a</sup>, Jiao Yin <sup>c</sup> and Chuanyi  
Wang <sup>c</sup>

<sup>a</sup> College of Chemistry and Chemical Engineering, Xinjiang Normal University, Urumqi,  
830054 Xinjiang, China;

<sup>b</sup> School of Environment and Guangdong Key Laboratory of Environmental Pollution  
and Health, Jinan University, Guangzhou 510632, China;

<sup>c</sup> Laboratory of Environmental Sciences and Technology, Xinjiang Technical Institute  
of Physics & Chemistry, and Key Laboratory of Functional Materials and Devices for  
Special Environments, Chinese Academy of Sciences, Urumqi 830011, China.

\*Corresponding author E-mail addresses: xyfan @jnu.edu.cn (X. Fan),

## **Experimental section**

### **1.1 Sample characterization**

X-ray diffraction (XRD) patterns of the samples were recorded by a Bruker D8 Advance X-ray diffractometer equipped with a diffracted-beam monochromator set for Cu K $\alpha$  radiation ( $\lambda = 1.5418 \text{ \AA}$ ) in the angular range between  $10^\circ$  and  $70^\circ$ . The morphologies of KBX were observed on a scanning electron microscope (SEM) using a ZEISS SUPRA55VP apparatus and energy dispersive X-ray (EDX) spectroscopy analysis were conducted by EDX8000. An infrared spectrum was recorded on Shimadzu IRAffinity-1 Fourier transform infrared spectrometer (FTIR) in the  $400\text{--}4000 \text{ cm}^{-1}$  range. The Optical UV-vis diffuse reflectance spectra (DRS) of samples were measured at room temperature by the Shimadzu Solidspec-3700 DUV spectrometer using standard BaSO<sub>4</sub> as a reference for baseline correction in the range from 200 to 800 nm. Before BET analysis, the samples were degassed at  $180^\circ\text{C}$  for 3 h by N<sub>2</sub> adsorption-desorption isotherms recorded at 77 K with a QUADRASORB IQ, Quantachrome instrument Corp and then obtained the surface area of samples. Photoluminescence (PL) spectra were recorded on a Hitachi High-Tech F-7000 fluorescence spectrophotometer using an excitation wavelength of 245 nm. The intermediate products during 2-CP degradation were qualitatively analyzed by a liquid chromatography–mass spectrometry (LC–MS, Agilent 1290).

### **1.2 Photocatalytic activity tests**

High performance liquid chromatography (HPLC) (Ultimate 3000, Dionex) were carried out with a C18 column ( $4.6 \text{ mm} \times 250 \text{ mm}$ ). The mixture of methanol and

water [85/15(v/v)] was used as an effluent, and the flow rate was 0.5 mL/min with detector wavelength 273 nm, 282 nm and 293 nm for 2-CP, 2,4-DCP and 2,4,6-TCP, respectively.

### **1.3 Photocatalytic degradation experiments**

Photocatalytic activity measurements for KBX were conducted at room temperature. 50 mg of as-obtained samples were dispersed in 100 mL aqueous solution of CPs (2-CP, 2,4-DCP, 2,4,6-TCP) (50 mg/L) in a 250 mL glass beaker and magnetically stirred for 20 min in the dark to ensure adsorption equilibrium and be fully dispersed among the photocatalyst. Then irradiate the reactor with light of a 300 W xenon lamp ( $\lambda > 200$  nm). The intensity of the light on solution system was measured by a spectroradiometer (300 mW/cm<sup>2</sup>). After a given irradiation time, sample was withdrawn from the reactor periodically (every two minutes) and the catalysts were separated from the suspension by a pinhole filter for further measurements by HPLC. The percentage of residual CPs solution at a selected time of irradiation is given by  $C/C_0$ , where  $C_0$  and  $C$  is the concentration of the CPs solution at the initial stage and selected irradiation time, respectively. For comparison, blank experiments were performed under the same conditions. In order to ensure the reproducibility of the experimental results, the photocatalytic activity tests were repeated three times.

### **1.4 Second harmonic generation (SHG) tests**

Second harmonic generation (SHG) tests of KBX powder by the Kurtz-Perry method. In general, since SHG efficiency has been shown to be strongly dependent

on particle size, KBX is ground and sieved into different particle size ranges, 38-55, 55-88, 88-105, 105-150 and 150-200  $\mu\text{m}$ . About 100 mg of powdered KBX was pressed into pellets, and the sample was irradiated with a pulsed infrared beam (10 ns, 15 kHz) generated by a Qswitched Nd:YAG laser having a wavelength of 1064 nm. Furthermore, in order to make a relevant comparison with known SHG materials, microcrystalline  $\text{KH}_2\text{PO}_4$  (KDP) was used as a reference and sieved to the same particle size range. A 532 nm filter was placed to absorb the fundamental wave between the crystal and the energy meter to block the basic light, and the visible light was transmitted to the photomultiplier tube, and the SHG signal was observed using a digital oscilloscope.

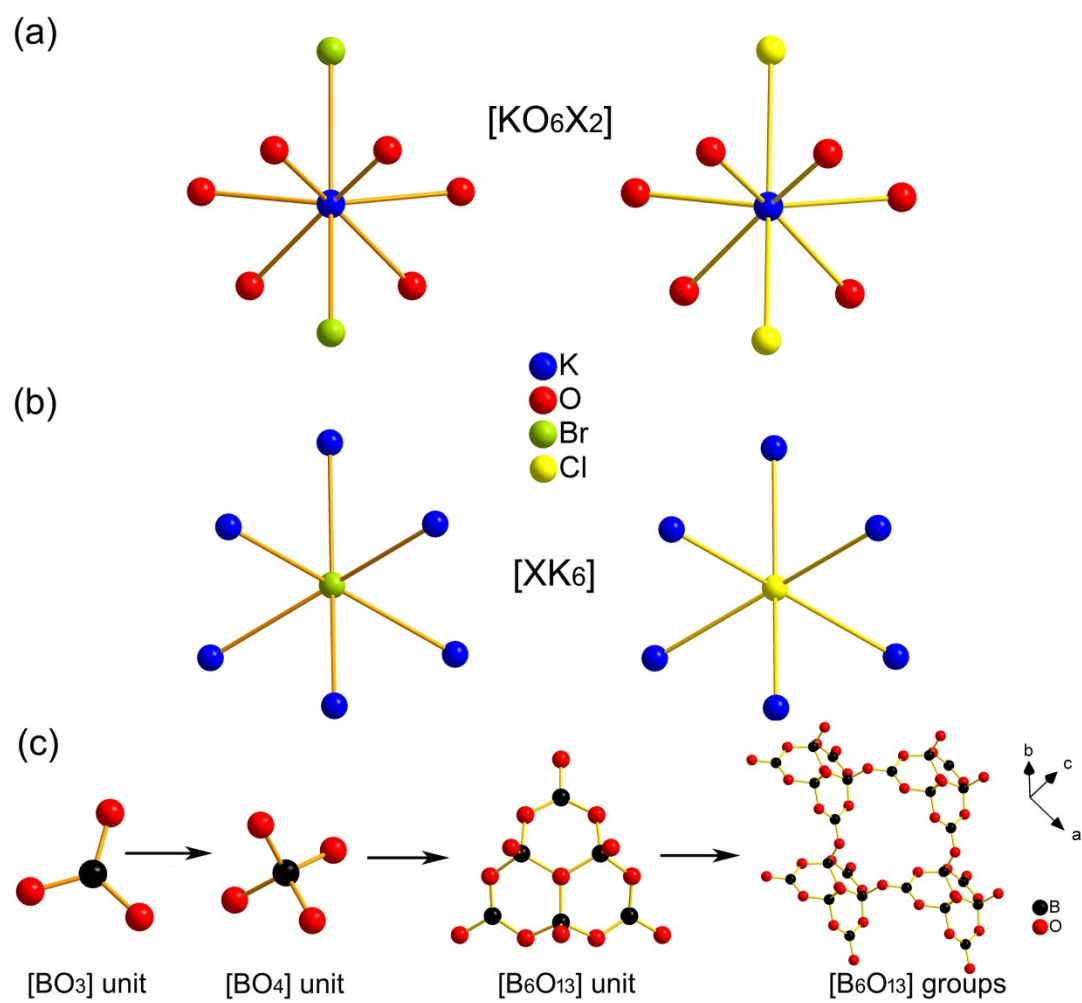


Fig. S1 Crystal structures of (a)  $[\text{KO}_6\text{X}_2]$  unit, (b)  $[\text{XK}_6]$  unit, and (c) the  $\text{BO}_3$  unit,  $\text{BO}_4$  unit,  $\text{B}_6\text{O}_{13}$  unit and four  $\text{B}_6\text{O}_{13}$  groups.

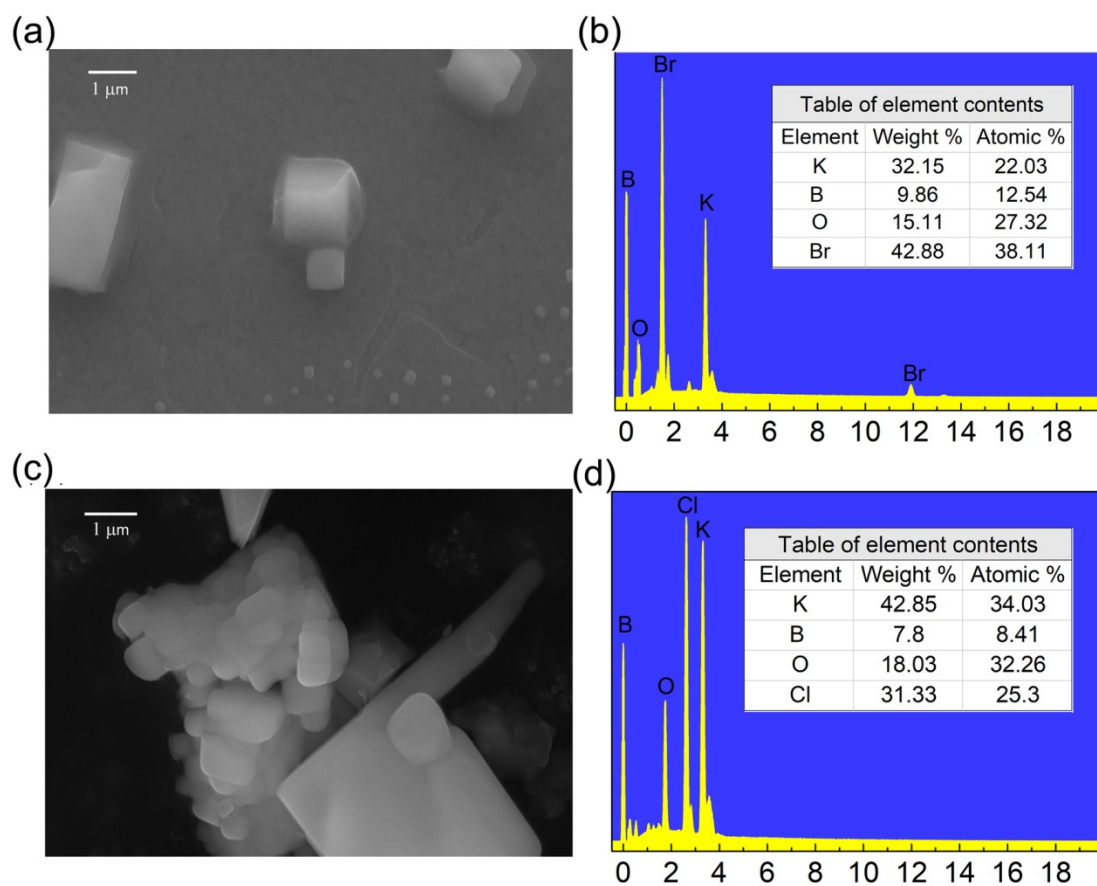


Fig. S2 SEM images of (a) KBB and (c) KBC samples; and EDX spectra for the samples (b) KBB and (d) KBC.

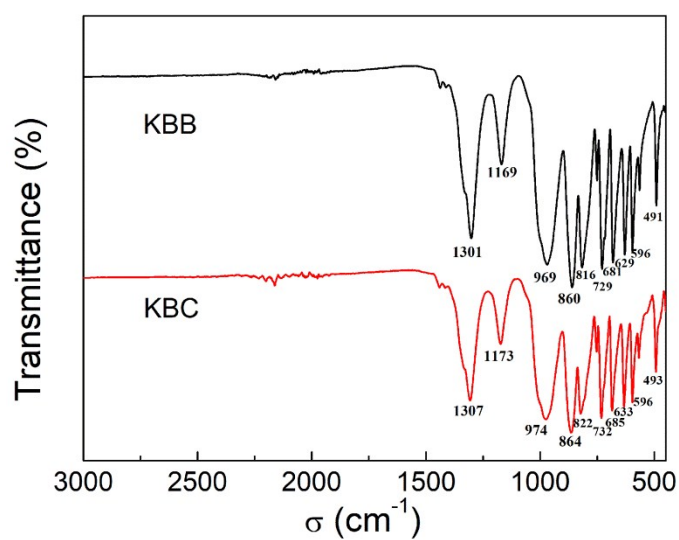


Fig. S3 Infrared spectroscopy of powder samples KBB and KBC.

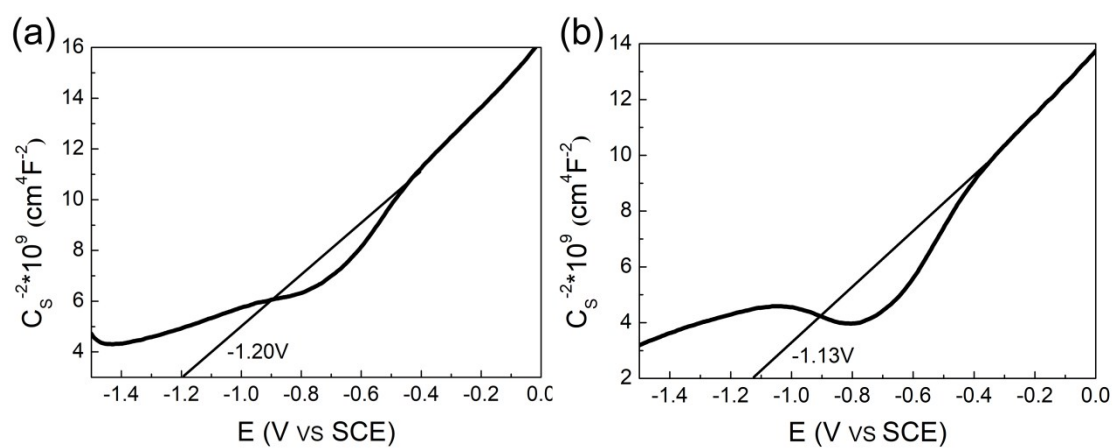


Fig. S4 Mott - Schottky plots for the powder samples of (a) KBB and (b) KBC.

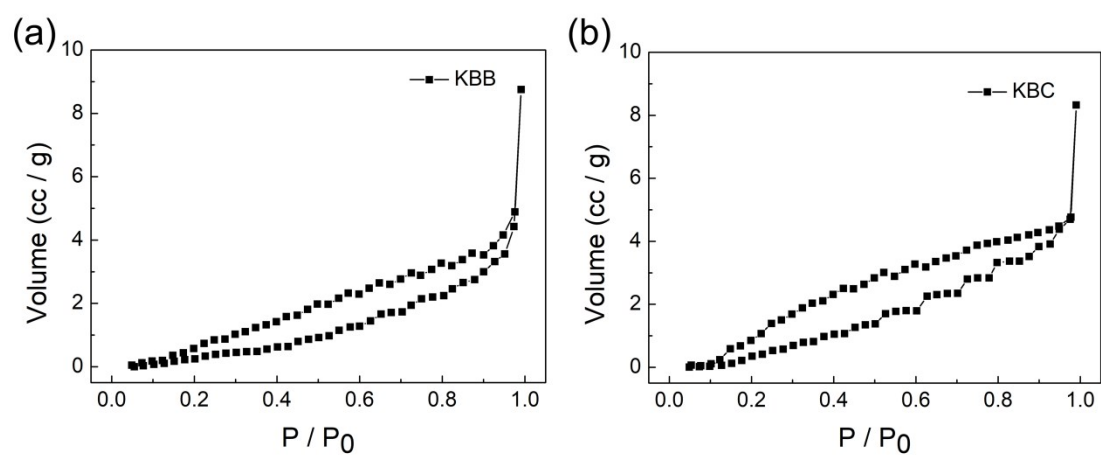


Fig. S5 Nitrogen adsorption-desorption isotherms of the (a) KBB and (b) KBC samples.

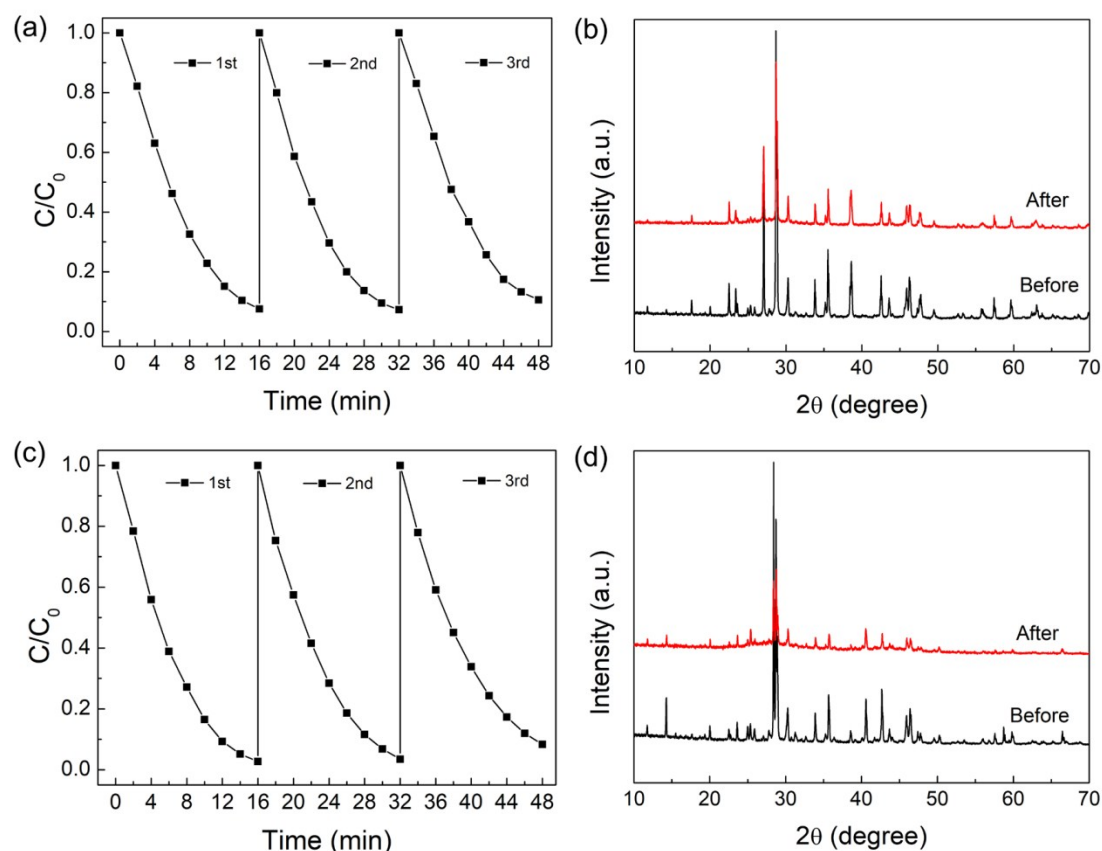


Fig. S6 Repeated experiments for the decomposition of 2-CP by KBB (a) and KBC (c) powder under UV light irradiation; and the XRD pattern of KBB (b) and KBC (c) before and after three cycles degradation of 2-CP.

The stability is of importance for its actual application. Three cycles of photocatalytic degradation experiments of 2-CP were conducted. Approximately 3.1% and 5.7% of degradation efficiency was decreased for KBC and KBB after three-cycle experiments (Figs. S6(a) and S6(c)). Further, no significant difference was observed in the XRD pattern after three cycles of the dechlorination reaction (Figs. S6(b) and S6(d)), demonstrating the stability of the KBX samples.



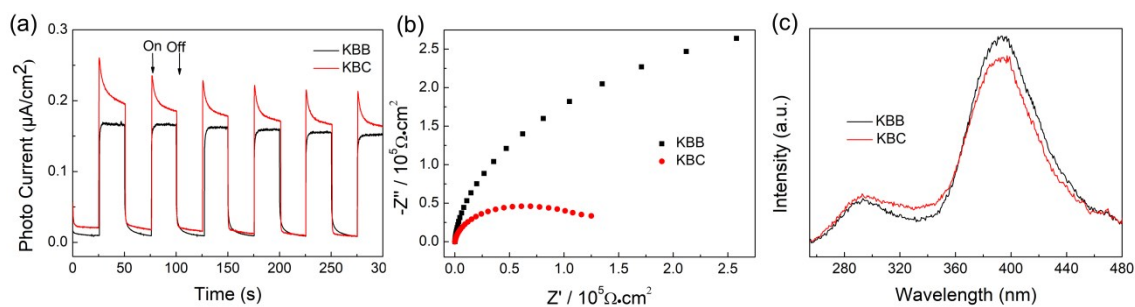


Fig. S7 (a) Photocurrent response; (b) Nyquist plots of electrochemical impedance spectrum of KBB and KBC samples; (c) The solid powder fluorescence tests of KBB and KBC samples;

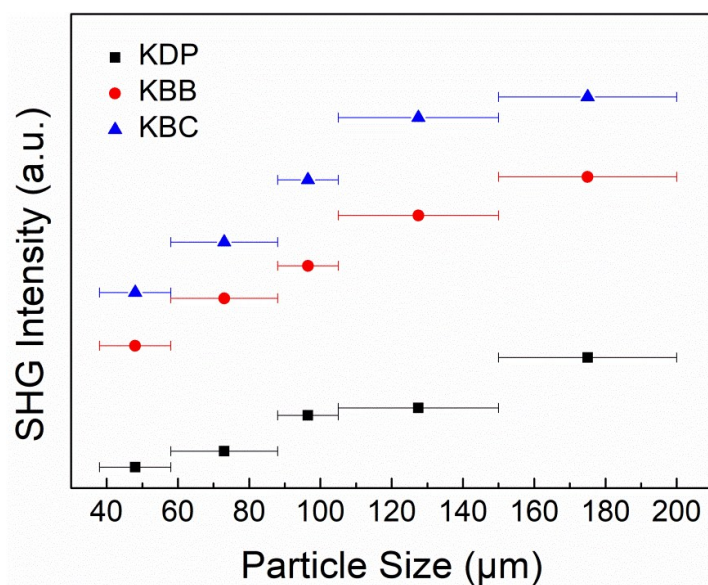


Fig. S8. The SHG measurement of KBX material and KDP.

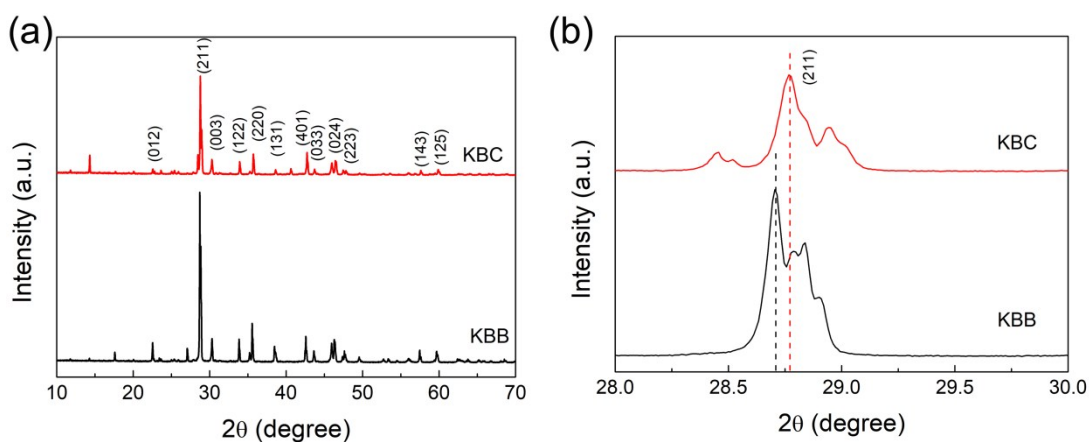


Fig. S9. (a) XRD patterns of the KBX samples. (b) The (211) peaks of the KBX samples at higher magnification.

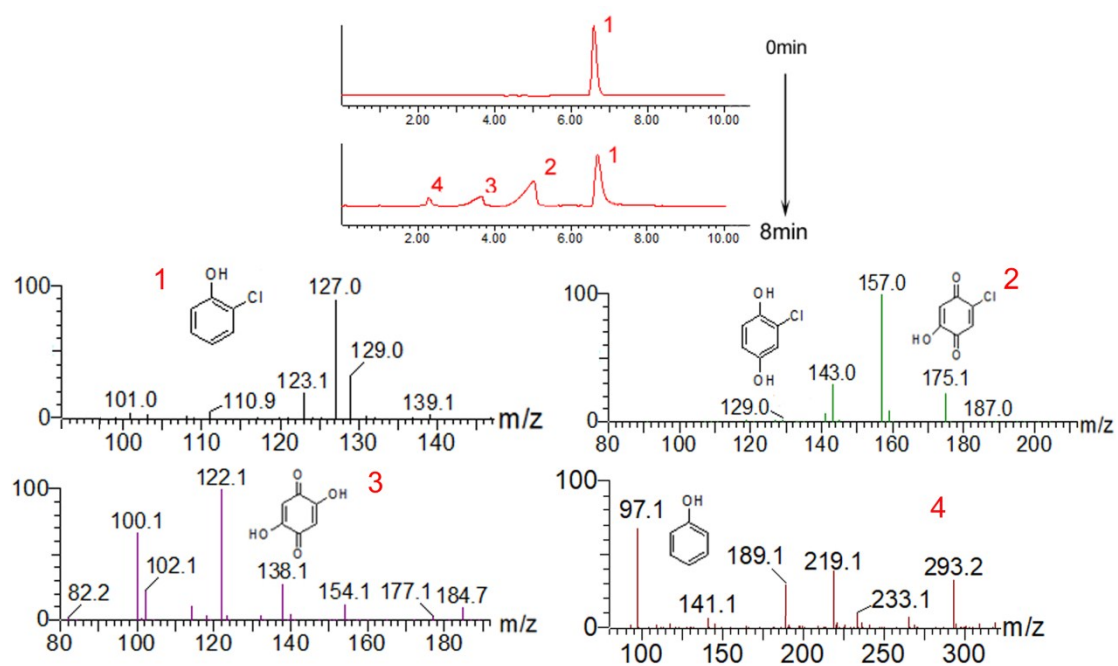


Fig. S10. LC-MS of 2-CP ( $R_t \approx 6.64 - 6.68$  min) by using KBC sample under UV light irradiation.

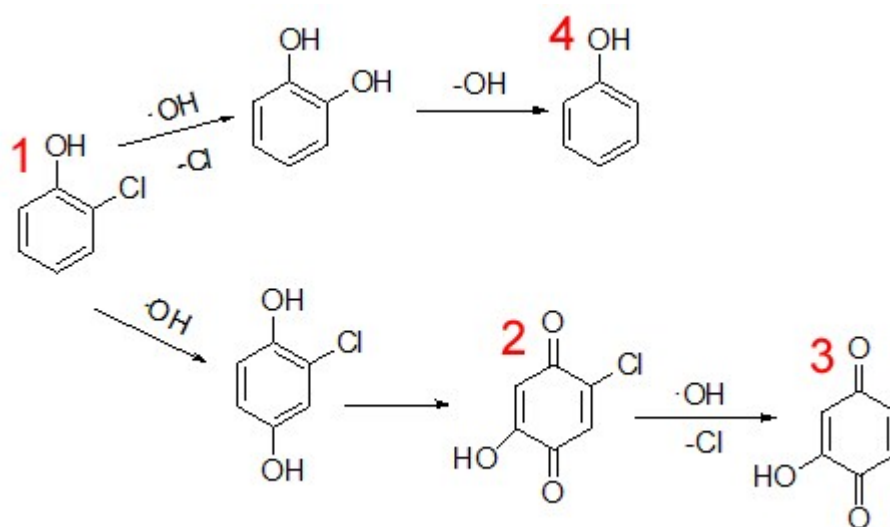


Fig. S11 The proposed pathway for 2-CP photo-dechlorination of KBC sample.

Table S1 The assignment of infrared spectra for KBX materials.

KBB (cm <sup>-1</sup> )	KBC (cm <sup>-1</sup> )	Assignment
1301, 1169	1307, 1173	asymmetric stretching vibrations of BO <sub>3</sub>
969	974	symmetric stretching vibrations of BO <sub>3</sub>
860, 816	864, 822	asymmetric and symmetric stretching vibrations of BO <sub>4</sub>
681, 629, 596	685, 633, 596	out-of-bending of BO <sub>3</sub>
567, 491	562, 493	bending of BO <sub>3</sub> and BO <sub>4</sub>

Table S2 The calculation details of band structures for KBX materials.

	$\lambda$ (nm)	X (eV)	E <sub>g</sub> (eV)	E <sub>VB</sub> (eV)	E <sub>CB</sub> (eV)
KBB	319	5.85	3.89	3.29	-0.60
KBC	328	5.87	3.78	3.26	-0.52

Table S3 LC-MS data of photodegraded products of 2-CP using KBC sample.

Retention time (min)	Mw (m/z)	Assignment
6.677	127	2-chlorophenol
2.21	97	phenol
3.76	122.1	2-hydroxy-1.4-benzoquinone
4.86	157	2-chloro-5-hydroxycyclohexa-benzoquinone
4.97	143	2-chloro-hydroquinone